Functionally and morphologically distinct populations of extracellular vesicles produced by human neutrophilic granulocytes

Ákos M. Lőrincz*, Maria Schütte*, Csaba I. Timár*, Daniel S. Veres[†], Ágnes Kittel[‡], Kenneth R. McLeish[§], Michael L. Merchant[§], Erzsébet Ligeti*

*Department of Physiology, Semmelweis University, Budapest, Hungary

[†]Department of Biophysics and Radiation Biology, Semmelweis University, Budapest, Hungary

[‡]Institute of Experimental Medicine of the Hungarian Academy of Sciences, Budapest, Hungary

[§]Department of Medicine, University of Louisville, Louisville, KY, USA

Summary sentence: Characterization of distinct properties, protein distribution profiles and function of extracellular vesicles released upon receptor stimulation or during spontaneous death of neutrophils

Running title: Distinct populations of PMN extracellular vesicles

Corresponding author: Erzsébet Ligeti M.D., PhD.

Professor of Physiology

Department of Physiology, Semmelweis University

1094, Budapest, Tűzoltó u. 37-47, Hungary

phone: +361 459 1500 ext. 60457

email: Ligeti@puskin.sote.hu

Ligeti.Erzsebet@med.semmelweis-univ.hu

Key words: apoptotic bodies, microparticles, microvesicles, bacterial survival, spontaneous death, protein profile

Total character count: 23 341

Total number of figures: 5

color figures: 0

references: 38

words in the Abstract: 171

words in summary sentence: 22

Abbreviations

Ab: Antibody

aEV: Opsonized particle induced extravellular vesicles

CD11b: Cluster definition 11b, Integrin alpha M

DLS: Dynamic Light Scattering

DMEM: Dulbecco's Modified Eagle's medium

EM: Electron Microscopy

emPAI: Exponentially Modified Protein Abundance Index

EV: Extracellular vesicles

HBSS: Hank's balanced salt solution

LTF: Lactoferrin

PI: Propidium iodide

PBS: Phosphate buffered saline

PMA: Phorbol-myristate-acetate

PMN: Polymorphonuclear cell

PS: Phosphatidylserine

ROS: Reactive oxygen species

SEM: Standard error of the mean

sEV: Spontaneous formed extravellular vesicles

SOD: Superoxide dismutase

Abstract

Extracellular vesicles (EVs) released during spontaneous death of human neutrophils were characterized and their properties compared to previously described EVs with antibacterial effect (aEV). The two vesicle populations overlapped in size and in part of the constituent proteins, both were stained with annexin V, were impermeable for propidium iodide but none of them produced superoxide. In contrast, remarkable differences were observed in the morphology, abundance of proteins and antibacterial function. EVs formed spontaneously in 30 min were more similar to EVs released during spontaneous death in one to three days, than to EVs formed in 30 min upon stimulation of opsonin receptors. Spontaneously generated EVs had no antibacterial effect in spite of their large number and protein content. We hypothesize two parallel mechanisms: one that proceeds spontaneously and produces EVs without antibacterial effect and another process that is triggered by opsonin receptors and results in differential sorting of proteins into EVs with antibacterial capacity. Our results call the attention to functional and morphological heterogeneity within the microvesicle/ ectosome fraction of EVs.

Introduction

Cells produce different types of extracellular vesicles (EVs) [1, 2], even prokaryotes are secreting EVs [3]. Exosomes are released by fusion of the membrane of the multivesicular bodies, a specialized endosomic compartment, with the plasma membrane. They are of the smallest size, around or below 100 nm [4-7]. Microvesicles/ microparticles/ ectosomes are generated by shedding from the plasma membrane [8-10]. These vesicles are generally larger than the exosomes, although their size represents a continuous spectrum [11]. Apoptotic vesicles, released by apoptotic cells, are regarded as the largest population of EVs, but neither their size nor their composition has been well characterized [9, 12-14].

Neutrophilic granulocytes (PMN) are short-lived cells that undergo spontaneous death within a couple of days both *in vivo* and *in vitro* under cell culture conditions [15-20]. In previous studies PMN-derived EV formation has been shown by several groups [21-26]. We and others demonstrated that both the composition and the function of EVs generated from isolated PMN in short-term incubation depend on the type of stimulus applied [25, 26] Specifically, opsonized particles induced the generation of EVs that were able to impair the growth of bacteria whereas EVs released upon soluble stimuli did not have any antibacterial effect [25] . We also observed spontaneous formation of EVs, both from isolated and from circulating PMN that lacked the antibacterial effect [25].

The aim of the present work was to investigate the EVs generated during spontaneous death of PMN and to define their relation to the EV types described earlier.

Materials and Methods

Materials

Annexin V-FITC was from BD Biosciences (New Jersey, USA), propidium iodide (PI) was from Invitrogen (Eugene,Oregon, USA), Saponin was from Merck (Darmstadt, Germany), Zymozan A, phorbolmyristate-acetate (PMA), lucigenin, ferricytochrome *c* (horse heart, type VI), superoxide dismutase (SOD) ovalbumin and DMEM from Sigma (St. Louis, MO, USA), sterile endotoxin-free HBSS from Thermo Scientific (Waltham, MA, USA), Ficoll from Phadia (Uppsala, Sweden). All other reagents were of research grade.

Preparation of EVs from PMN

Venous blood was drawn from healthy adult volunteers according to procedures approved by the Institutional Review Board of the Semmelweis University. Neutrophils were obtained by dextran sedimentation followed by Ficoll-Paque gradient centrifugation as described previously [27]. The preparation contained over 95% PMN and less than 0.5% eosinophils.

For production of antibacterial EVs PMN (typically 10^7cells) were incubated with opsonized Zymozan A particles (5 mg added in 100 μL HBSS) for 30 min at 37 °C on a linear shaker (80 rpm/min). After incubation, PMN were sedimented (500 x *g*, Hermle Z216MK 45° fixed angle rotor, 5 minutes, 4°C) and the supernatant was filtered through a 5 μm pore sterile filter (Sterile Millex Filter Unit, Millipore, Billerica, MA, USA). The filtered fraction was sedimented again (15 700 x *g*, Hermle Z216MK 45° fixed angle rotor, 10 minutes, 4°C). The sediment was suspended in HBSS at the original incubation volume. Spontaneously produced EVs were isolated similar to aEV without Zymozan A activation.

Spontaneous cell death was initiated in DMEM medium at 37°C by the presence of 5% CO_2 [18, 19]. EVs were collected and isolated after 1, 2 and 3 day incubation. The remaining

cells were labelled with propidium iodide and FITC-annexin V and analysed by flow cytrometry.

RNA extraction

RNA was extracted with the TriPure isolation reagent (Roche Applied Science, Penzberg, Germany) according to manufacturer's instructions. The presence and amount of RNA were measured with Nano Drop (Thermo Fisher Scientific, Wilmington, DE, USA).

Opsonization of Zymozan A and S. aureus

5 mg Zymozan A or 4.5 x 10^8/mL *S. aureus* (ATCC: 29213) was opsonized with 100 µL pooled normal human serum for 30 minutes at 37°C. After opsonization, the particles were centrifuged (8 000 x *g*, Hermle Z216MK 45° fixed angle rotor, 10 minutes, 4°C), and washed in HBSS.

EV detection by flow cytometry

EVs were labeled with a monoclonal Ab against the alpha chain of the major PMN integrin (anti-CD11b-RPE, 1µg/mL, Dako, Glostrup, Denmark) for 30 minutes at 37°C then washed in HBSS. For flow cytometric characterization a Becton Dickinson FACSCalibur flow cytometer was used. The procedure of measurement is detailed in Pure HBSS medium was used for setting the threshold to eliminate instrument noise. In the next step fluorescent beads (3.8 µm SPHERO Rainbow Alignment Particles from Spherotech Inc., Lake Forest, IL, USA) were detected. The upper size limit of EV detection range was set to include the signals from the beads. Although the PMN-derived EVs are mostly below 800 nm [25], we chose a significantly broader size range to detect larger apoptotic bodies as well. The smallest fluorescent particles reliably detected by a conventional cytometer could be around 300 nm [28]. The fluorescent gate was set above the signal of the isotype antibody labelled EVs. PMN-derived EVs were enumerated and characterized in the fluorescent gate above. To confirm the vesicular nature of detected events

1% TritonX-100 detergent was used to solubilize vesicles [29]. Non-solubilized events (around 5 %) were subtracted. To avoid swarm detection flow rate was held below 1000 events/s.

Electron microscopy of EV

Pelleted EVs were fixed at room temperature for 60 minutes with 4% paraformaldehyde in PBS. The preparations were postfixed in 1% OsO4 (TAAB Laboratories Equipment Ltd, Aldermaston, England) for 30 minutes. After rinsing with distilled water, the pellets were dehydrated by ethanol, including by block staining with 1% uranyl-acetate in 50% ethanol for 30 minutes, and embedded in Taab 812 (TAAB Laboratories Equipment Ltd, Aldermaston, England). After overnight polymerization at 60°C and sectioning for electron microscopy, the ultrathin sections were analyzed with a Hitachi 7100 electron microscope equipped by Veleta, a 2k x 2k MegaPixel side-mounted TEM CCD camera (Olympus,Center Valley, PA, USA). Contrast and brightness of electron micrographs were edited by Adobe Photoshop CS3 (Adobe Photoshop Incorporation,San Jose, CA, USA).

Dynamic Light Scattering (DLS)

DLS measurements were performed at room temperature with an equipment consisting of a goniometer system (ALV GmbH, Langen, Germany), a diode-pumped solid-state laser light source (Melles Griot 58-BLS-301, 457 nm, 150 mW) and a light detector (Hamamatsu H7155 PMT module). The evaluation software yielded the autocorrelation function of scattered light intensity which was further analyzed by the maximum entropy method (MEM), and from where the different contributions of this function were determined.

Measurement of bacterial survival

EV samples in HBSS were incubated with ($2.5x10^7$/mL) opsonized *S. aureus* for 40 minutes at 37°C. Samples were taken at starting point and 40 min later. Samples were lysed in ice-cold HBSS containing 1 mg/mL saponin and frozen at -80°C for 20 minutes then thawed to inactivate EVs. Freezing did not impair subsequent growth of *S. aureus*. Lysed samples were diluted in Lysogeny Broth (LB medium; 10 g tryptone, 5 g yeast extract, 10 g NaCl in 1L water, pH adjusted to 7.0 with NaOH), then bacteria were grown in a shaking plate reader (Labsystems iEMS, Thermo Scientific, Waltham, MA, USA) at 37°C for 8 hours, and the OD was followed continuously at 650 nm, as described earlier [27]. Samples were run in 8 parallels.

Measurement of $O_2^{\bullet-}$ -production

The rate of $O_2^{\bullet-}$ -production was determined as the superoxide-dismutase-sensitive portion of ferricytochrome *c* reduction measured at 550 nm in a Labsystem iEMS microplate reader as described earlier [27].

Mass Spectrometry Analysis

EV samples (45 μg) were lysed using 2% sodium dodecyl sulfate (SDS) at 65°C for 30 min, reduced, alkylated, and digested using trypsin (Promega, Madison, WI, USA) as previously described [30] with modifications for the filter assisted sample preparation (FASP) protocol [31]. Prior to trypsinization samples were pipetted into a Microcon-10 Ultracel YM-10 10,000 NMWL centrifugal filter (Millipore) and rinsed (3X) using 250uL of 8M urea / 0.1M Tris-HCl pH 8.5 to remove SDS. Prior to digestion the sample was diluted to 0.8 M urea/0.1M Tris-HCl pH 8.5. Peptides isolated through the YM-10 filter were desalted and concentrated using NEST Group C18 PROTO™ UltraMicroSpin columns. Desalted samples were separated offline into seven strong cation exchange (SCX) fractions using SCX MicroTrapTM (Michrom-Bruker, Auburn, CA, USA) prior to analysis by 1D-RP (C18) nanoflow UHPLC and nanoelectrospray-MS as

describe previously [32] on the Thermo LTQ-Orbitrap ELITE MS platform.

Data were acquired using Oribtrap ELITE in ETD decision tree method. All MS1 was acquired with the FTMS and MS2 acquired with the ITMS. All MS data were searched using PD1.4 with Sequest and Mascot (v2.4) in a decoy database search strategy against UniprotKB *Homo sapiens* reference proteome canonical and isoform sequences current as of 7/22/14. Searches were performed with a fragment ion mass tolerance of 1.2 Da and a parent ion tolerance of 50 ppm. Iodoacetamide derivative of cysteine was specified as a fixed modification. Oxidation of methionine was specified as a variable modification.

Search data results file were imported into Scaffold (v4.3.4Proteome Software Inc., Portland, OR) to control for <1.0% FDR with Peptide and Protein Prophet. Peptide identifications were accepted if they could be established at greater than 95.0% probability by the Peptide Prophet algorithm [33]. Protein identifications were accepted if they could be established at greater than 95.0% probability assigned by the Protein Prophet algorithm [34]. Quantitative assessment and comparison of EV protein composition with different stimuli was based on a spectral counting-based approach.

Immunoblotting

EV were lysed in 4x Laemmli sample buffer (252 mM Tris-HCl, 40% glycerin, 8% Sodium Dodecyl Sulfate, 0,04% bromephenol blue, 4% β-mercaptoethanol, pH 6,8), boiled, run on 10% (w/v) polyacrylamide gels and transferred to nitrocellulose membranes. After blocking for 1 h in PBS containing 5% albumin and 0.1% (w/v) Tween 20, blots were incubated with anti-lactoferrin polyclonal antibody in 1:1000 dilution or anti-β-actin mAb (both from Sigma, St. Louis, USA) in 1:10000 dilution in PBS containing 5% ovalbumin. Bound antibody was detected with enhanced chemiluminescence using horseradish peroxidase-conjugated anti-rabbit-Ig (from donkey) or anti-mouse-Ig (from sheep) secondary antibodies (GE Healthcare,

LittleChalfont, Buckinghamshire, UK) used in 1:5000 dilution.

Statistics

Statistical analysis was performed with STATISTICA 8.0 software (Statsoft Inc. Tulsa, OK, USA) with two-sample *t*-test. All samples were compared to sEV. Results were considered significant at a (two sided) p value less than or equal to 0.05 (signed as * or #).

Results

EV production during spontaneous death of PMN

First we compared the properties of PMN isolated freshly or kept in cell culture medium for a few days. PMN were regarded healthy if they could not be stained either with annexin V or propidium iodide (PI). As summarized in Fig. 1A, freshly isolated PMN were 95% healthy and only 5% showed annexin V binding. On the first day majority of the cells (55%) did bind annexin V indicating enrichment of phosphatidylserine (PS) on their surface. Approx. 30% of the cells proved to be healthy and only 10% was PI-positive, i.e. sufficiently leaky to enable PI to enter the nucleus. On the second and later days PMN positive both for annexin V and PI predominated.

Next we investigated the number and overall composition of EVs produced in short (30 min) or in longer term incubations in cell culture medium. The number of detectable EVs increased dramatically as the count of healthy PMN decreased (Fig. 1B). On the 3rd day EVs outnumbered the initial PMN count tenfold. The protein content of spontaneously formed vesicles was about ten times higher after 1 day (1st day EV) than after 30 min incubation (sEV), but did not further increase on the following days (Fig. 1C). Accordingly, the protein content per vesicle showed significant decrease from sEV to EVs released during 3 days of culture (Fig. 1D). Antibacterial EVs (aEV) were significantly more numerous and contained more protein than sEVs did, although both vesicles were generated in 30 min (Fig. 1C).

Morphological properties of different PMN-derived EV populations

The size of different PMN-derived EV populations was first investigated by dynamic light scattering (DLS) (Fig. 2A). The two populations of EVs formed in short incubation (sEV and aEV) did not differ in size and they showed two maximums around 100 and 500 nm. The size

scattering distribution curve for EVs issued from spontaneously dying cells was shifted to the right and the peaks were around 200 and 800 nm.

Next we investigated the EVs by electron microscopy (Fig. 2B-F). All the fractions contained heterogeneously sized vesicles surrounded by intact membrane. There were however differences in the density of the vesicle content. The frequency of densely packed vesicles was the highest in the aEV fraction (Fig. 2B). This is in accordance with their high protein content per vesicle. EVs generated by spontaneously dying PMN exhibited increasing number of empty looking large vesicles (Fig. 2D-F), consistent with the decreasing protein content per vesicle (Fig. 1D).

Protein composition of different PMN-derived EV populations

Our detailed proteomic analysis identified 798 unique proteins with 2 peptides and 95% confidence (Table S1). First, we investigated protein overlap between the 3 most characteristic populations: aEV, sEV, 1st day of spontaneous death (Fig. 3A). A total of 274 proteins were present in all 3 populations. In addition, 324 proteins were shared between sEV and 1st day EV, the two types of spontaneously formed EVs. Thus, a total of 598 proteins were shared by sEV and 1st day EV. In contrast, aEV shared only 10 additional proteins with sEV (for a total of 284 common proteins) and 7 with 1st day EV population (for a total of 281 common proteins). The 1st day EV fraction contained 112 unique proteins whereas only 7 proteins were specifically distributed to aEV.

Next we listed the proteins in all 5 populations in decreasing order of abundance. Figures 3B and 3C present a graphical representation of that distribution. Comparison of the abundance rank between sEV and 1st day EV (two populations of spontaneously formed EVs) gave a symmetrical distribution suggesting that the two vesicle populations contained the same proteins in similar relative quantities. In contrast, comparing the abundance rank of aEV with sEV (two

populations of short-term generated EVs) resulted in asymmetrical distribution indicating significant differences in the relative amount of constituting proteins.

Similar graphs were created for each possible pair of vesicle populations and the obtained square of the coefficients of multiple correlation (R^2) are summarized in Fig. 3D. The mathematical analysis clearly shows that the protein pattern is more similar between all the EV populations formed spontaneously than between any spontaneously formed vesicle population and the activation-induced aEV population.

Next we compared the amount of specific proteins with distinct localization to neutrophils and role in PMN functions among the 5 EV populations (Fig. 4). We reported previously that granule proteins were enriched in aEV as compared to sEV [25]. The present study confirmed the difference in EV expression of granule proteins between aEV and sEV (Fig 4A-C). Surprisingly, the amount of granule proteins was also increased in EVs released from spontaneouly dying cells (Fig. 4A). In Western blots, an increase in the amount of lactoferrin could be detected, whereas the amount of actin did not change significantly, resulting in a clear and gradual increase in the lactoferrin to actin ratio from sEV towards EVs released from spontaneously dying PMN (Fig. 4C).

Finally we investigated the presence of the subunits of the NADPH oxidase (Fig. 4D). As previously observed, aEV did not contain two essential cytosolic components ($p47^{phox}$ and $p40^{phox}$) [25]. In contrast, all the spontaneously formed EV populations contained all 6 subunits.

Functional properties of different PMN-derived EV populations

At last we investigated two major PMN functions: superoxide production and impairment of bacterial growth (Fig. 5). In both cases we tested intact neutrophils as positive control. The strongest stimulation of superoxide production can be reached by the pharmacological agent phorbol-myristate-acetate (PMA). As demonstrated in Fig. 4A, even this agent was not able to

induce any detectable superoxide generation in any of the EV populations. No superoxide was detectable with more sensitive, luminescent techniques, either (data not shown).

In the bacterial survival test, 18% of the initial bacteria survived in the presence of intact PMN and approx. 60% in the presence of aEV generated from the same number of PMN (Fig. 4B). In contrast, sEV did not impair bacterial survival, and bacteria even grew in the presence of EVs released from PMN cultured for 3 days. It should be noted that both the number and protein content of the applied "3rd day EV" fraction was significantly higher than that of the aEV fraction (see Fig. 1C).

Discussion

Our detailed analysis revealed that some properties were shared by all investigated PMN-derived EV populations (Table 1): they were all stained by annexin V, and PMN characteristic marker (CD11b), contained RNA, had a heterogeneous size distribution and they shared approx. 50% of the identified proteins. On the other hand, none of them was stained by PI and none of them was able to produce superoxide. In addition to the similarities, there were important differences, in the morphological properties, protein composition and in the antibacterial capacity. Comparing the properties and composition of the 5 investigated EV populations indicates that the 4 spontaneously formed EV types are more similar to each other than any of them to aEV, the vesicles induced by receptor activation.

On the basis of these findings we propose that EVs are formed from PMN by (at least) two distinct mechanisms. One is a spontaneously propagating process that produces an increasing number of EVs with decreasing protein content per vesicle as cells proceed to spontaneous death. This could also be a neutrophil-specific property related to the short life-span of these cells. The spontaneously formed vesicles have no antibacterial function. The other mechanism is initiated by opsonin receptors and produces EVs with high protein content and definitive antibacterial capacity. In our proteomic analysis we could reveal only few proteins with low abundance that were specific for aEVs, whereas 290 proteins were shared with spontaneously formed vesicles (Fig. 3A). However, there were significant differences in the abundance of these shared proteins (Fig. 3B-D) suggesting a selective sorting mechanism [5, 35]. The importance of differential protein sorting in EV formation is supported by the surprising pattern of NADPH oxidase subunits. Despite the presence of membrane bound subunits and other cytosolic members, two essential cytosolic activators are completely missing from aEVs (Fig.4B). There was no ROS production in the spontaneously formed vesicles either, perhaps due

to inhomogeneous vesicle composition or lack of signaling elements (Fig 5A). This highlights how carefully ROS production is controlled even during cell death [36]. The fact that only aEVs were able to impair bacterial growth - in spite of high granule protein content in EVs from spontaneously dying PMNs – clearly indicates that the quantity of granule proteins by itself does not determine the biological activity of EVs. The large quantity of granule proteins in EVs produced during spontaneous death may be a mechanism for sequestered removal of the dangerous granule enzymes packed in vesicles with "eat me" signals as PS [15, 37].

Beyond the observations specifically relevant for neutrophilic granulocytes, our results demonstrate that many easily and widely determined properties were similar between EVs formed in short-term incubations or during spontaneous cell death. The size distribution of vesicles released from cultured PMN was shifted towards higher values, supporting the notion that apoptotic vesicles are larger, but the size range was widely overlapping (Fig. 2A). Staining properties and nucleic acid content were similar and a large number of proteins were shared (Table 1 and Fig. 3A). Our data indicate that similar to the exosome fraction [38], EVs sedimented in the microvesicle/ ectosome fraction are also heterogenous and the boundary between specifically triggered EVs and apoptotic bodies is not sharp. On the basis of our results protein amount per vesicle, electron microscopic images and mainly specific biological functions may be useful in distinguishing various EV types.

Authorship

A.M.L.: designed and carried out most of the experiments, prepared figures and wrote part of the manuscript

M.S.: participated in experiments determining the number, protein content and antibacterial effect of different EV populations

Cs.I.T.: established the methodology of EV preparation and detection of antibacterial effect

D.S.V.: carried out the DLS measurements

Á.K.: carried out the electron micrographs

K.R.M: analyzed proteomic data

M.L.M: performed the mass spectrometry and analyzed proteomic data

E.L.: directed and financed the experiments, organized discussions, wrote and edited the manuscript

Acknowledgements

The authors are indebted to Professor Edit Buzás and Mr. X. Osteikoetxea for stimulating discussions and Ms. Regina Tóth-Kun and Edit Fedina for devoted and expert technical assistance. Experimental work was financially supported by Hungarian Research Fund (OTKA K 108382).

Conflict of Interest Disclosure

None of the authors has any conflict of interest to disclose.

References

1. Thery, C., Zitvogel, L., Amigorena, S. (2002) Exosomes: composition, biogenesis and function. Nature reviews. Immunology 2, 569-79.
2. Raposo, G. and Stoorvogel, W. (2013) Extracellular vesicles: exosomes, microvesicles, and friends. The Journal of cell biology 200, 373-83.
3. Mashburn, L. M. and Whiteley, M. (2005) Membrane vesicles traffic signals and facilitate group activities in a prokaryote. Nature 437, 422-5.
4. Bobrie, A., Colombo, M., Raposo, G., Thery, C. (2011) Exosome secretion: molecular mechanisms and roles in immune responses. Traffic 12, 1659-68.
5. Colombo, M., Moita, C., van Niel, G., Kowal, J., Vigneron, J., Benaroch, P., Manel, N., Moita, L. F., Thery, C., Raposo, G. (2013) Analysis of ESCRT functions in exosome biogenesis, composition and secretion highlights the heterogeneity of extracellular vesicles. Journal of cell science 126, 5553-65.
6. Colombo, M., Raposo, G., Thery, C. (2014) Biogenesis, secretion, and intercellular interactions of exosomes and other extracellular vesicles. Annual review of cell and developmental biology 30, 255-89.
7. Johnstone, R. M. (2006) Exosomes biological significance: A concise review. Blood cells, molecules & diseases 36, 315-21.
8. Buzas, E. I., Gyorgy, B., Nagy, G., Falus, A., Gay, S. (2014) Emerging role of extracellular vesicles in inflammatory diseases. Nature reviews. Rheumatology 10, 356-64.
9. Gyorgy, B., Szabo, T. G., Pasztoi, M., Pal, Z., Misjak, P., Aradi, B., Laszlo, V., Pallinger, E., Pap, E., Kittel, A., Nagy, G., Falus, A., Buzas, E. I. (2011) Membrane vesicles, current state-of-the-art: emerging role of extracellular vesicles. Cellular and molecular life sciences : CMLS 68, 2667-88.
10. Zwaal, R. F. and Schroit, A. J. (1997) Pathophysiologic implications of membrane phospholipid asymmetry in blood cells. Blood 89, 1121-32.
11. Heijnen, H. F., Schiel, A. E., Fijnheer, R., Geuze, H. J., Sixma, J. J. (1999) Activated platelets release two types of membrane vesicles: microvesicles by surface shedding and exosomes derived from exocytosis of multivesicular bodies and alpha-granules. Blood 94, 3791-9.
12. Crescitelli, R., Lasser, C., Szabo, T. G., Kittel, A., Eldh, M., Dianzani, I., Buzas, E. I., Lotvall, J. (2013) Distinct RNA profiles in subpopulations of extracellular vesicles: apoptotic bodies, microvesicles and exosomes. Journal of extracellular vesicles 2.
13. Turiak, L., Misjak, P., Szabo, T. G., Aradi, B., Paloczi, K., Ozohanics, O., Drahos, L., Kittel, A., Falus, A., Buzas, E. I., Vekey, K. (2011) Proteomic characterization of thymocyte-derived microvesicles and apoptotic bodies in BALB/c mice. Journal of proteomics 74, 2025-33.
14. Sadallah, S., Eken, C., Schifferli, J. A. (2011) Ectosomes as modulators of inflammation and immunity. Clinical and experimental immunology 163, 26-32.
15. Savill, J. S., Wyllie, A. H., Henson, J. E., Walport, M. J., Henson, P. M., Haslett, C. (1989) Macrophage phagocytosis of aging neutrophils in inflammation. Programmed cell death in the neutrophil leads to its recognition by macrophages. The Journal of clinical investigation 83, 865-75.
16. Luo, H. R. and Loison, F. (2008) Constitutive neutrophil apoptosis: mechanisms and regulation. American journal of hematology 83, 288-95.

17. Savill, J. and Haslett, C. (1995) Granulocyte clearance by apoptosis in the resolution of inflammation. Seminars in cell biology 6, 385-93.
18. Tortorella, C., Piazzolla, G., Spaccavento, F., Pece, S., Jirillo, E., Antonaci, S. (1998) Spontaneous and Fas-induced apoptotic cell death in aged neutrophils. Journal of clinical immunology 18, 321-9.
19. Colotta, F., Re, F., Polentarutti, N., Sozzani, S., Mantovani, A. (1992) Modulation of granulocyte survival and programmed cell death by cytokines and bacterial products. Blood 80, 2012-20.
20. McCracken, J. M. and Allen, L. A. (2014) Regulation of human neutrophil apoptosis and lifespan in health and disease. Journal of cell death 7, 15-23.
21. Mesri, M. and Altieri, D. C. (1999) Leukocyte microparticles stimulate endothelial cell cytokine release and tissue factor induction in a JNK1 signaling pathway. The Journal of biological chemistry 274, 23111-8.
22. Mesri, M. and Altieri, D. C. (1998) Endothelial cell activation by leukocyte microparticles. Journal of immunology 161, 4382-7.
23. Gasser, O. and Schifferli, J. A. (2004) Activated polymorphonuclear neutrophils disseminate anti-inflammatory microparticles by ectocytosis. Blood 104, 2543-8.
24. Gasser, O., Hess, C., Miot, S., Deon, C., Sanchez, J. C., Schifferli, J. A. (2003) Characterisation and properties of ectosomes released by human polymorphonuclear neutrophils. Experimental cell research 285, 243-57.
25. Timar, C. I., Lorincz, A. M., Csepanyi-Komi, R., Valyi-Nagy, A., Nagy, G., Buzas, E. I., Ivanyi, Z., Kittel, A., Powell, D. W., McLeish, K. R., Ligeti, E. (2013) Antibacterial effect of microvesicles released from human neutrophilic granulocytes. Blood 121, 510-8.
26. Dalli, J., Montero-Melendez, T., Norling, L. V., Yin, X., Hinds, C., Haskard, D., Mayr, M., Perretti, M. (2013) Heterogeneity in neutrophil microparticles reveals distinct proteome and functional properties. Molecular & cellular proteomics : MCP 12, 2205-19.
27. Rada, B. K., Geiszt, M., Kaldi, K., Timar, C., Ligeti, E. (2004) Dual role of phagocytic NADPH oxidase in bacterial killing. Blood 104, 2947-53.
28. van der Pol, E., van Gemert, M. J., Sturk, A., Nieuwland, R., van Leeuwen, T. G. (2012) Single vs. swarm detection of microparticles and exosomes by flow cytometry. Journal of thrombosis and haemostasis : JTH 10, 919-30.
29. Gyorgy, B., Modos, K., Pallinger, E., Paloczi, K., Pasztoi, M., Misjak, P., Deli, M. A., Sipos, A., Szalai, A., Voszka, I., Polgar, A., Toth, K., Csete, M., Nagy, G., Gay, S., Falus, A., Kittel, A., Buzas, E. I. (2011) Detection and isolation of cell-derived microparticles are compromised by protein complexes resulting from shared biophysical parameters. Blood 117, e39-48.
30. Uriarte, S. M., Rane, M. J., Merchant, M. L., Jin, S., Lentsch, A. B., Ward, R. A., McLeish, K. R. (2013) Inhibition of neutrophil exocytosis ameliorates acute lung injury in rats. Shock 39, 286-92.
31. Wisniewski, J. R., Zougman, A., Nagaraj, N., Mann, M. (2009) Universal sample preparation method for proteome analysis. Nat Methods 6, 359-62.
32. Baba, S. P., Hoetker, J. D., Merchant, M., Klein, J. B., Cai, J., Barski, O. A., Conklin, D. J., Bhatnagar, A. (2013) Role of aldose reductase in the metabolism and detoxification of carnosine-acrolein conjugates. J Biol Chem.
33. Keller, A., Nesvizhskii, A. I., Kolker, E., Aebersold, R. (2002) Empirical statistical model to estimate the accuracy of peptide identifications made by MS/MS and database search. Anal Chem 74, 5383-92.
34. Uriarte, S. M., Powell, D. W., Luerman, G. C., Merchant, M. L., Cummins, T. D., Jog, N. R., Ward, R. A., McLeish, K. R. (2008) Comparison of proteins expressed on secretory

vesicle membranes and plasma membranes of human neutrophils. Journal of immunology 180, 5575-81.
35. Timar, C. I., Lorincz, A. M., Ligeti, E. (2013) Changing world of neutrophils. Pflugers Archiv : European journal of physiology 465, 1521-33.
36. Decoursey, T. E. and Ligeti, E. (2005) Regulation and termination of NADPH oxidase activity. Cellular and molecular life sciences : CMLS 62, 2173-93.
37. Erwig, L. P. and Henson, P. M. (2008) Clearance of apoptotic cells by phagocytes. Cell death and differentiation 15, 243-50.
38. Bobrie, A., Colombo, M., Krumeich, S., Raposo, G., Thery, C. (2012) Diverse subpopulations of vesicles secreted by different intracellular mechanisms are present in exosome preparations obtained by differential ultracentrifugation. Journal of extracellular vesicles 1.

Legends to Figures

Figure 1. ***Basic properties of initiating cells and released vesicle populations.***

A. Viability changes of PMN population in a 3 day incubation; **B.** Cell count (left axis) decrease and EV production (right axis) during 3 day incubation; **C.** Comparison of number (left axis) and protein content (right axis) of freshly produced EVs to spontaneous death derived EVs; **D.** Comparison of protein content per vesicle of different type EVs. (Bars represent SEM; n=3, in case of protein measurements n=5).

Figure 2. ***Morphology of different vesicle populations.***

A. Size distribution spectra of EVs measured by DLS. sEV represented by black line, 3rd day EV represented by broken line; **B-F.** Representative electron microscopic images of aEV (**B**), sEV (**C**), 1st day EV (**D**), 2nd day EV (**E**), 3rd day EV (**F**). Original magnification is 30 000x.

Figure 3. ***Protein distribution profile of different vesicle populations*****.**

A. Protein distribution identified by mass spectrometry in aEV, sEV and 1st day EV; **B.** Spot diagram on proteins identified by mass spectrometry ranked according their abundance in sEV (x axis) and in 1st day EV (y axis); **C.** Spot diagram on proteins identified by mass spectrometry ranked according their abundance in sEV (x axis) and in aEV (y axis); **D.** Heat diagram of each R^2 value determined by protein rank correlation (showed in panel **B** and **C**).

Figure 4. ***Analysis of specific proteins in different vesicle populations*****.**

A. Amount (emPAI values) of all identified granule proteins related to actin; **B.** Representative Western blot of lactoferrin and actin; **C.** Densitometric analysis of lactoferrin related to actin (+ SEM; n=4); **D.** EmPAI values of NADPH oxidase subunits in different EV samples.

Figure 5. ***Functional properties of different vesicle populations.***

A. Superoxide production of EVs and control PMNs after PMA stimulation; **B.** Effect of EVs and PMNs on bacterial growth after a 40 minutes co-incubation. 100% represents the initial bacterial count. (n=4, or 8 in case of 3rd day EV +SEM).

Table I. ***Comparison of the properties of different PMN-derived EV types***

	Mother cell staining	**PS expression**	**PI staining**	**PMN specific markers**	**EM**	**Size**	**ROS production**	**Antibacterial effect**	**RNA**
aEV	$AnnV^-$ Pi^-	+	-	+	Dens, intact	Peaks: 100, 500 nm	-	+	+
sEV	$AnnV^-$ Pi^-	+	-	+	Dens, intact	Peaks: 100, 500 nm	-	-	+
1st, 2nd, 3rd day EV	$AnnV^+$ Pi^+	+	-	+	Empty, intact	Peaks: 200, 800 nm	-	-	+

Figure 1.

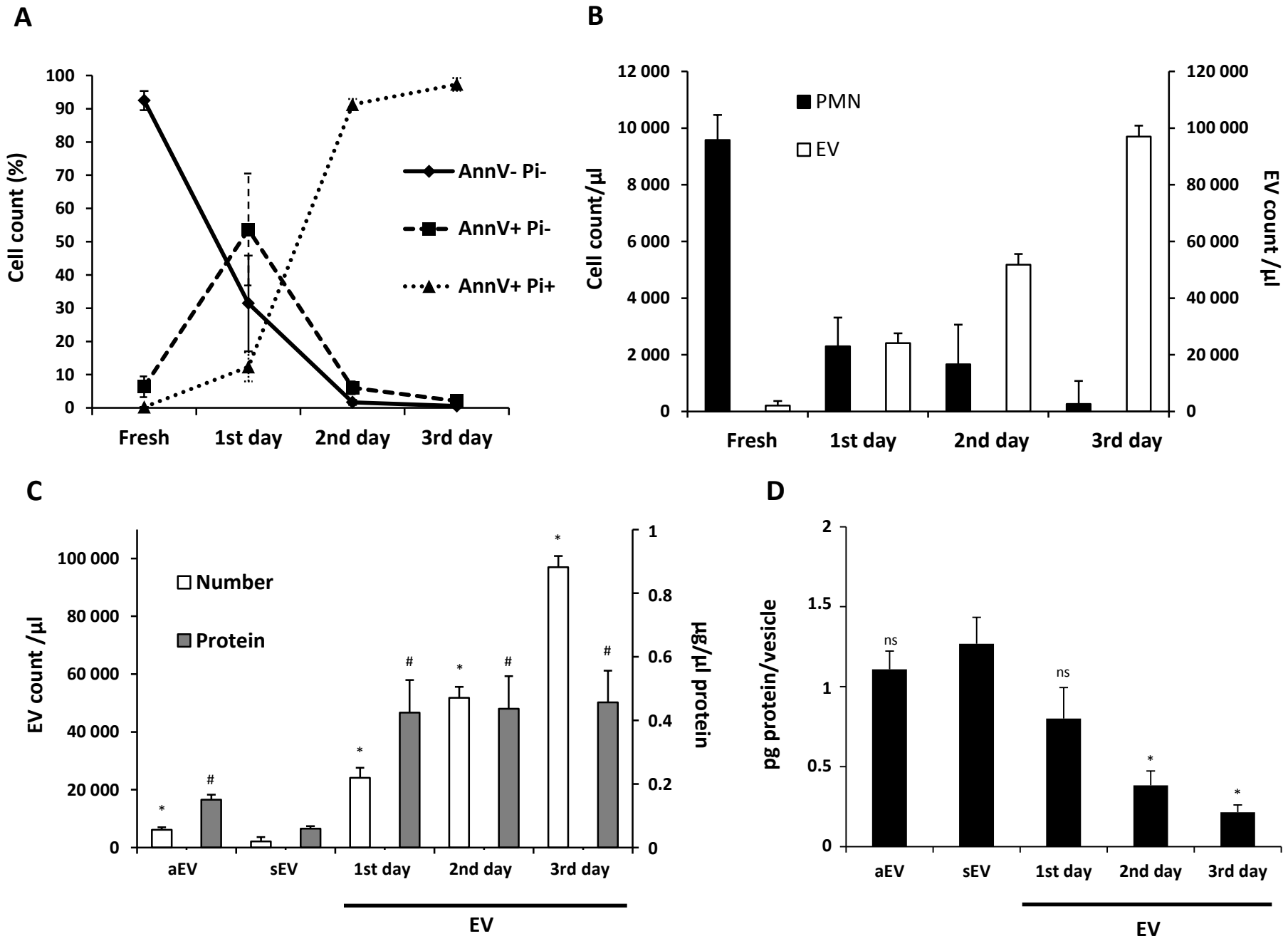
A
Cell count (%)
AnnV- Pi-
AnnV+ Pi-
AnnV+ Pi+
Fresh
1st day
2nd day
3rd day
B
Cell count/µl
EV count /µl
PMN
EV
C
EV count /µl
µg/µl protein
Number
Protein
aEV
sEV
1st day
2nd day
3rd day
EV
D
pg protein/vesicle
ns
aEV
sEV
1st day
2nd day
3rd day
EV

Figure 2.

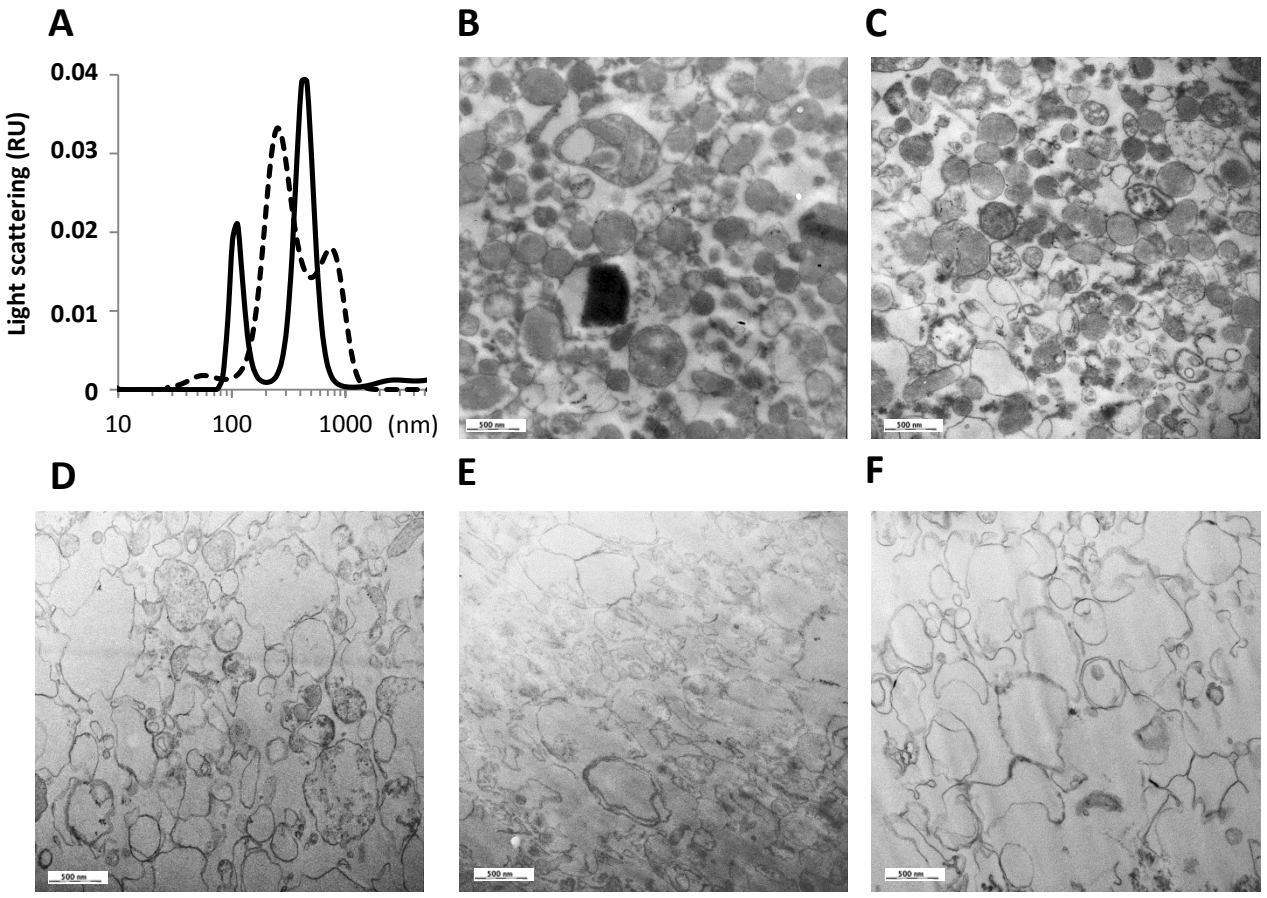
A
B
C
D
E
F
0.04
0.03
0.02
0.01
0
Light scattering (RU)
10
100
1000
(nm)
500 nm

Figure 3.

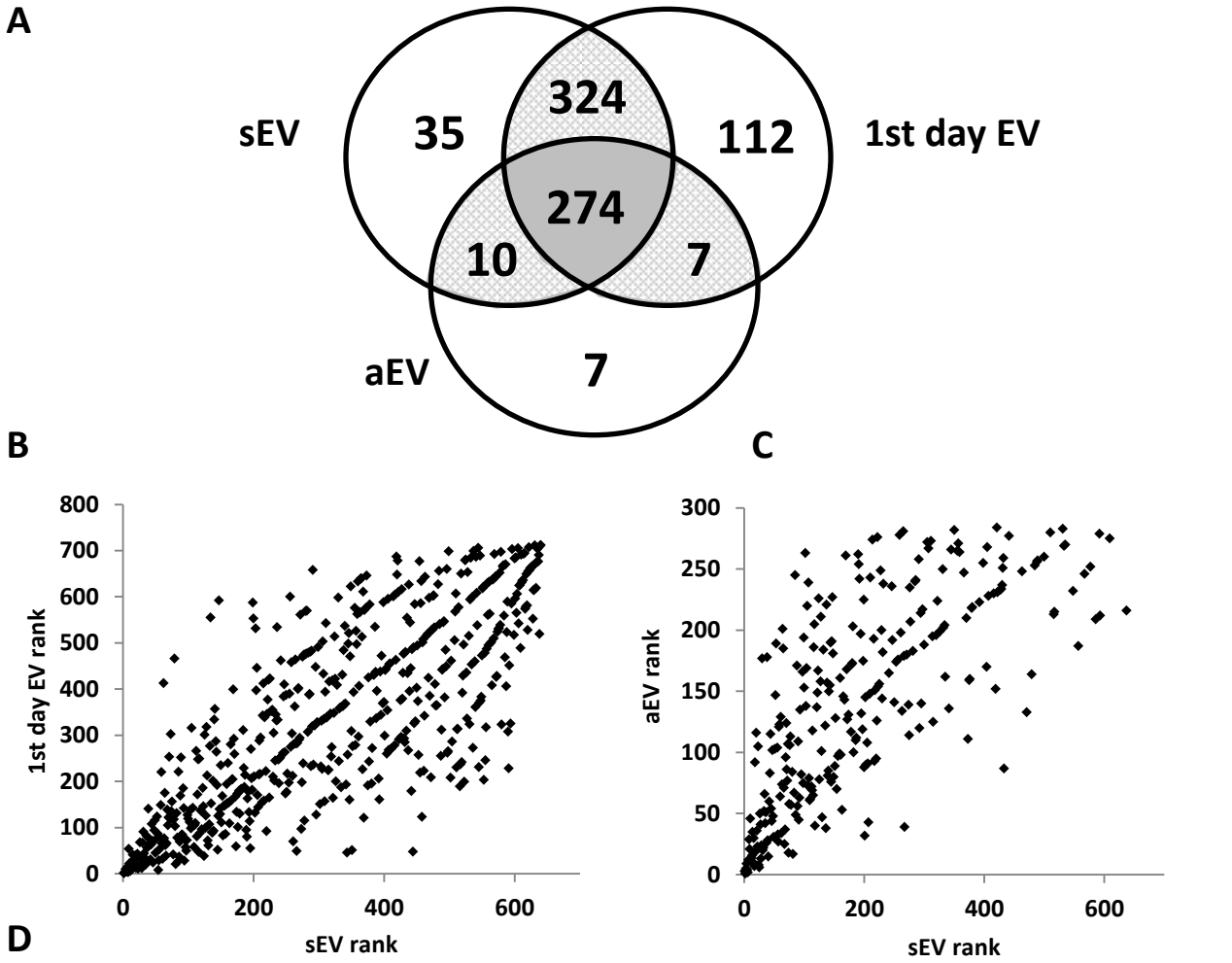

D

R^2	aEV	sEV	1st day EV	2nd day EV	3rd day EV
aEV	1	0.52	0.4	0.44	0.3
sEV	0.52	1	0.62	0.59	0.63
1st day EV	0.4	0.62	1	0.81	0.73
2nd day EV	0.44	0.59	0.81	1	0.78
3rd day EV	0.3	0.63	0.73	0.78	1

Figure 4.

A

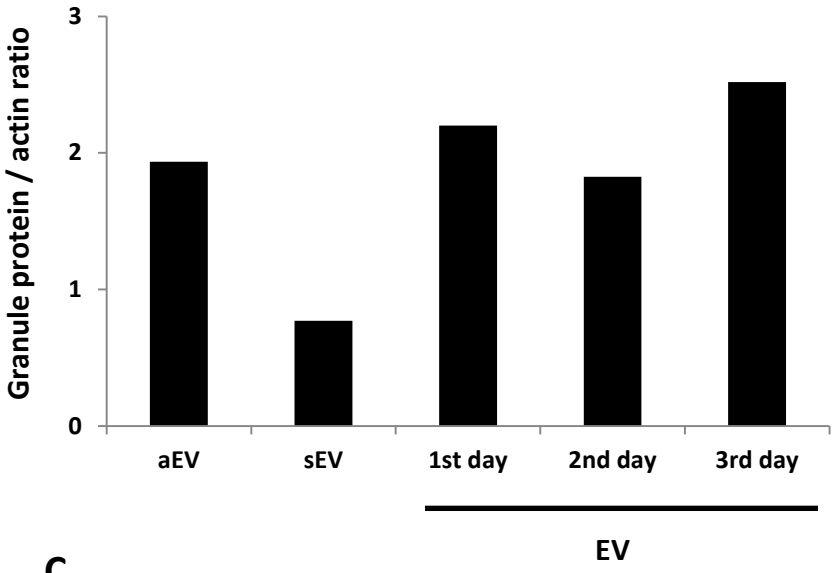

B

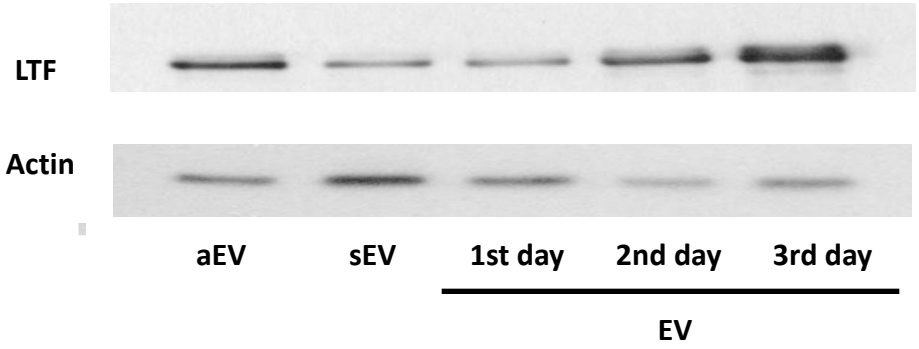

C

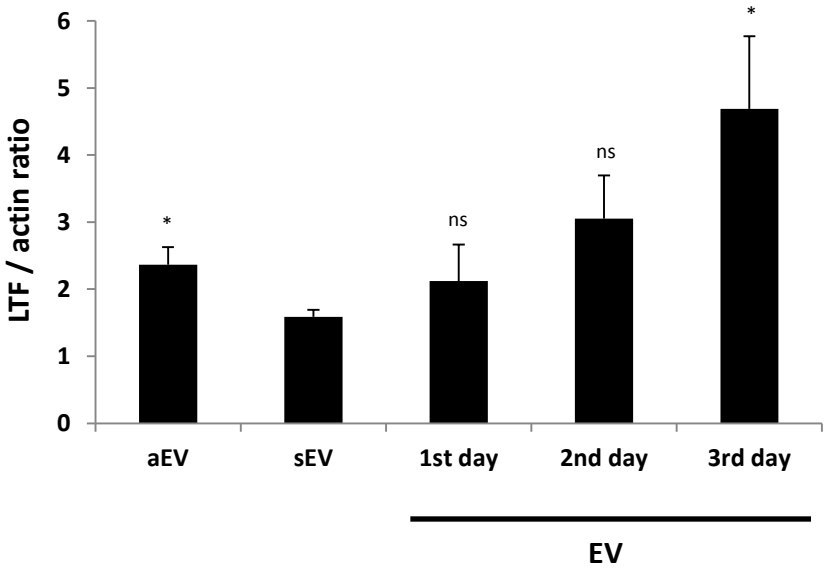

D

	gp91^{PHOX}	p22^{PHOX}	p67^{PHOX}	p47^{PHOX}	Rac1/2	p40^{PHOX}
aEV	0.77	0.78	0.12	-	4.96	-
sEV	0.68	0.68	0.14	0.40	5.22	0.22
1st day EV	0.35	0.41	0.23	0.77	3.37	0.13
2nd day EV	0.57	1.89	0.32	0.93	5.06	0.09
3rd day EV	0.44	0.57	0.17	0.83	3.00	0.12

Figure 5.

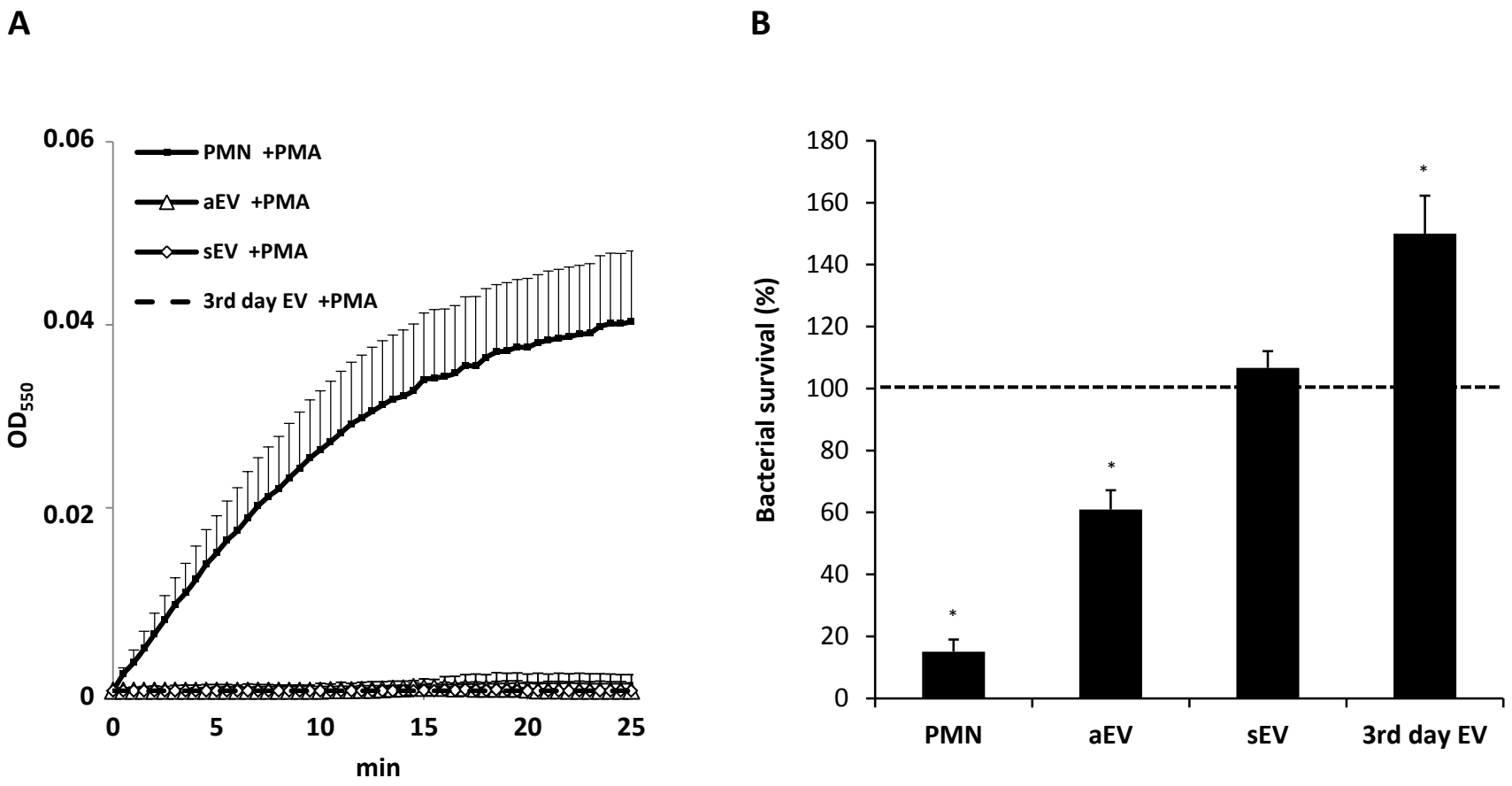
A
0.06
0.04
0.02
0
PMN +PMA
aEV +PMA
sEV +PMA
3rd day EV +PMA
OD550
0
5
10
15
20
25
min
B
180
160
140
120
100
80
60
40
20
0
Bacterial survival (%)
*
*
*
PMN
aEV
sEV
3rd day EV